The Chromophore Structural Changes during the Photocycle of Phytochrome: A Combined Resonance Raman and Quantum Chemical Approach

MARIA ANDREA MROGINSKI,*
DANIEL H. MURGIDA, AND
PETER HILDEBRANDT
Technische Universität Berlin, Institut für Chemie, Max-Volmer-Laboratorium für Biophysikalische Chemie, Sekr. PC 14, Strasse des 17, Juni 135, D-10623 Berlin, Germany

Received July 22, 2006

ABSTRACT
Phytochromes are sensory photoreceptors that, upon light irradiation, can be transformed between an inactive and an active state. The conversion is initiated by the photoisomerization of the cofactor, a linear methine-bridged tetrapyrrole, followed by conformational relaxations of the chromophore and the protein matrix that finally leads to the formation of the signaling state. To elucidate the underlying molecular processes, resonance Raman spectroscopy combined with quantum chemical calculations constitutes a powerful approach since it allows determination of the chromophore structure in the various states of phytochrome. On the basis of these studies, a molecular model for the photoinduced reaction cycle is derived.

Introduction

Phytochromes constitute a family of plant photoreceptors that regulate a variety of processes related to the growth of plants including the germination of seeds, the formation of leaves, and the time of flowering.[1] Although the various functions have been well-documented on a phenomenological level for a long time, little is known about the signaling pathways from the absorption of light to the cellular responses. Plant phytochromes are large 124-kDa proteins that include a light-sensing module in the N-terminal part and a regulatory module in the C-terminal region. The sensor module converts the light signal into a conformational change of the protein and thus activates the regulatory module, typically a histidine kinase domain, which then initiates subsequent processes downstream in various signal transduction cascades. Representatives of the phytochrome family have also been discovered in bacteria and fungi and here even the physiological function of the photoreceptor is yet enigmatic.[2]

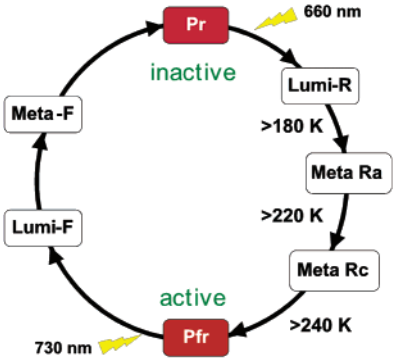

FIGURE 1. Reaction scheme of the photoinduced reaction cycle of phytochromes including the approximate temperatures at which the intermediate states can be cryogenically trapped.

Common to all phytochromes is that the sensor module binds a linear methine-bridged open-chain tetrapyrrole that upon light absorption undergoes a *Z*/*E* isomerization at the C−D methine bridge as the first step of the interconversion between two stable states (Figures 1 and 2).[3] These two states, denoted according to the absorption properties of the chromophore as red-absorbing (Pr) and far-red-absorbing state (Pfr), represent the nonactive or active state of the photoreceptor, which, hence, can be considered as an optical switch. The photoinduced reaction cycle involves various intermediates that have been detected in transient or low-temperature absorption spectroscopy. The formation of the first intermediate states (Lumi-R, Lumi-F) is associated with the chromophore photoisomerization. Subsequent relaxation processes linked to the formation and decay of the Meta states also include the protein environment. These protein conformational changes, which are still not identified, constitute the structural basis for the activation and deactivation of the photoreceptor. In this context, the recently published three-dimensional (3-D) structure of the Pr state is of utmost importance (Figure 3).[4] Although the structure was obtained from a phytochrome deletion mutant of *Deinococcus radiodurans* (DrBphP) that is not fully photoactive, it provides a detailed picture of the initial state of this phytochrome. However, the comparison with results obtained in spectroscopic studies also raises new questions. Specifically, the 3-D structure reveals a chromophore geometry of the Pr state (*ZZZssa*) that is

Maria Andrea Mroginski obtained her Ph.D in 2002 from the Universidad Nacional de La Plata for her theoretical and experimental work carried out at the Max Planck Institut für Strahlenchemie in Mülheim. After a postdoctoral stay at the Instituto de Tecnologia Química e Biológica (Universidade Nova de Lisboa), she moved to the Technische Universität Berlin where she has been appointed as staff scientist.

Daniel H. Murgida obtained his Ph.D. in chemistry in 1997 from the Universidad de Buenos Aires. In 1999, he joined the Max Planck Institute für Strahlenchemie as an Alexander-von-Humboldt fellow. In 2001, he was appointed as staff scientist at the Instituto de Tecnologia Química e Biológica (Universidade Nova de Lisboa). Since 2003, he has been Staff Scientist at the Technische Universität Berlin and Visiting Professor at ITQB.

Peter Hildebrandt received his Ph.D. in chemistry from the Universität Göttingen in 1985. After a postdoctoral stay in Princeton, he worked at the Max-Planck-Institutes in Göttingen and in Mülheim a.d.R. where he became staff scientist. In 2001, he was appointed as Investigador Coordenador at the Instituto de Tecnologia Química e Biológica (Universidade Nova de Lisboa). Since 2003, he has been a Full Professor for Physical Chemistry and Biophysical Chemistry at the Technische Universität Berlin and Visiting Professor at ITQB.

* To whom correspondence should be addressed. Tel: +49-30-314-21584. Fax: +49-30-314-21122. E-mail: andrea.mroginski@tu-berlin.de.

10.1021/ar6000523 CCC: $37.00
Published on Web 02/06/2007

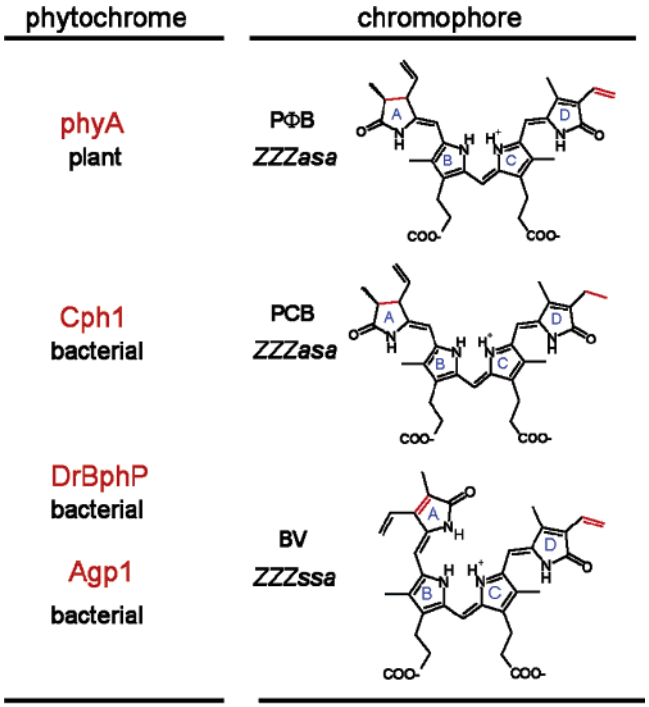

FIGURE 2. Various phytochromes and their natural chromophores phytochromobilin (PΦB), phycocyanobilin (PCB), and biliverdin (BV). The chemical differences between the chromophores are highlighted in red. The tetrapyrroles are bound to a cysteine side chain via the vinyl substituent of ring A. The geometry of the DrBphP cofactor is revealed by the crystal structure,[4] whereas for phyA, Cph1, and Agp1, the chromophore geometries are derived from the RR spectroscopic data as discussed in this work.

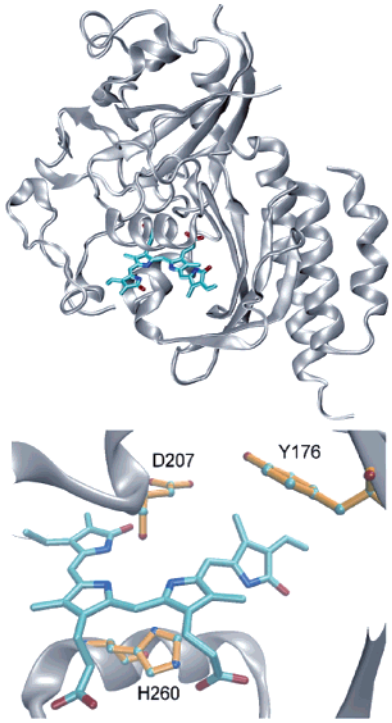

FIGURE 3. Crystal structure of the chromophore binding domain of DrBphP (top)[4] with the structure of the chromophore pocket shown in an enlarged view (bottom), highlighting the BV chromophore and the amino acids Asp207, Tyr176, and His260, corresponding to Asp197, Tyr166, and His250 in Agp1.

different from that derived from resonance Raman (RR) spectroscopy on plant phytochrome (*ZZZasa*).

This Account is dedicated to summarizing the current state of RR spectroscopic research on phytochromes. We will first outline the strategic concept of the combined experimental and theoretical approach to extract structural data from the RR spectra. The second part focuses on the determination of the methine bridge geometry and protonation state of the tetrapyrroles in the various states of phytochrome. On the basis of these results and the 3-D structure data of DrBphP, we present a model for the reaction mechanism of the photoinduced Pr to Pfr photoconversion. Finally, we will point out methodological developments that are relevant for future RR spectroscopic analyses of phytochromes.

Strategy for Resonance Raman Spectroscopic Studies of Phytochrome

To exploit the advantages of RR spectroscopy, the exciting laser line must be in resonance with an electronic transition of the phytochrome chromophore, which, however, inevitably induces the photoconversion. Thus, various intermediate states may be accumulated in the laser focus such that the resultant spectra are difficult to interpret. For other types of photoreceptors such as retinal proteins, this difficulty can be overcome by time-resolved RR experiments.[8,9] This approach, however, has not yet been employed for phytochrome since large amounts of sample and long measuring times are required due to the long photocycle period.[9]

Thus, RR spectroscopic studies of phytochrome are so far restricted to quasi-stationary conditions. In these experiments, the degree of photoconversion can be minimized by a second laser beam to drive the photoproduct back to the initial state.[10,11] An additional drawback of RR spectroscopic measurements in rigorous resonance with the first electronic transition (Q-band at ca. 700 nm) is the interference with fluorescence, which may largely obscure the RR bands. This problem can be overcome by employing the shifted-excitation difference technique that allows reconstruction of the RR bands after subtraction of the fluorescence background.[11]

Alternatively, one may use excitation lines in resonance with the second (nonfluorescent) electronic transition (Soret band at ca. 400 nm)[6,12] or near-infrared excitation lines that are on the long-wavelength side of the Q-band.[7,13−16] The 1064-nm line of the Nd:YAG laser is close enough to the Q-band to achieve a (pre)resonance enhancement of the chromophoric bands that allows for an effective discrimination of the Raman bands of the protein matrix. Under these conditions, no photochemical processes are induced by the excitation line such that "clean" spectra of the parent states are obtained in single-beam experiments. For probing the intermediate states, photoconversion is induced by an additional irradiation source while keeping the sample at a sufficiently low temperature to block the thermal decay of the desired intermediate (Figure 1). This cryogenic trapping usually leads to a

mixture of different states. Thus, residual spectral contributions from the nonphotolyzed parent state or other intermediates have to be subtracted from the measured spectrum to obtain a pure spectrum of the target state. Along this strategy, the RR spectra of all states of the photoinduced reaction cascade of plant phytochrome phyA (as depicted in Figure 1) have been measured.[13,14] The substantial differences between the RR spectra of the various states reflect the structural changes of the chromophore during the photoconversion. Extracting this structure information from the spectra, however, represents a considerable challenge.

We have employed a dual strategy by combining experimental and theoretical approaches. The experimental approach is directed to accumulate a large set of RR spectroscopic data by extending the studies to recombinant phytochrome adducts formed by wild-type proteins and genetically modified variants from different sources and various tetrapyrroles and their isotopomers.[14−18] The manifold of adducts arises from the fact that different members of the phytochrome family bind chemically different chromophores (Figure 2). The theoretical approach is based on scaled quantum mechanical force fields to calculate the Raman spectra for various tetrapyrrole geometries such that the comparison of calculated and experimental spectra then permits the identification of the chromophore structure in the respective phytochrome states.[19]

Quantum Chemical Calculations of Vibrational Spectra

The quantum chemical calculation of vibrational spectra of large molecules (∼100 atoms) is restricted to the harmonic approximation, which, as well as intrinsic deficiencies of the methods, causes errors of the force constants and thus distinct deviations of the calculated frequencies from the experimental values. Since these errors are largely systematic, scaling procedures can be employed for compensation. A physically substantiated method pioneered by Pulay and co-workers is based on scaling of the force field itself,[20] taking into account that the intrinsic errors are slightly different for force constants referring to different internal coordinates. This model further assumes that the scaling factors are transferable between different molecules with similar internal coordinates. Thus, these scaling factors can be optimized for a set of training molecules, for which a complete vibrational assignment is straightforward. This set of global scaling factors may then be extended to the molecules of interest, that is., the target molecules, without further adjustments.

On the basis of a variety of molecules, which represent structural motifs of methine-brigded tetrapyrroles, we have optimized scaling factors on the level of density functional theory (DFT) with the B3LYP hybrid functional and the 6-31G* basis.[21,22] It was found that 11 different scaling factors are required to achieve a satisfactory global

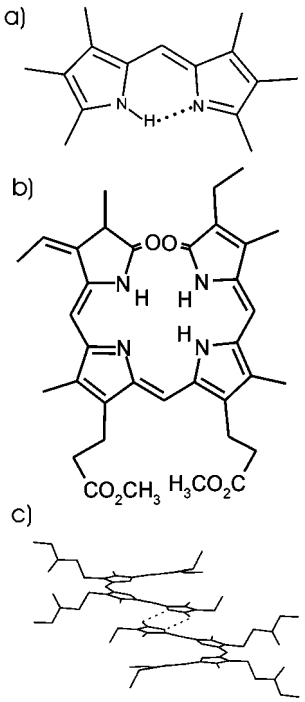

FIGURE 4. Structural formulas of (a) HMPM, (b) monomeric PCBE in the *ZZZsss* configuration, and (c) the DD PCBE dimer.

fit to the experimental spectra with a root-mean-square deviation for calculated frequencies of ca. 10 cm^{-1}.

The protein-bound tetrapyrroles are likely to be involved in a network of hydrogen bonds specifically via the N−H groups of the pyrrole nitrogens. Therefore, specific attention has to be paid to the effect of hydrogen-bond interactions on the vibrational spectra, particularly in view of the known deficiencies of quantum chemical methods in treating hydrogen-bonded systems.[23] In this respect, the methine-bridged dipyrrole hexamethylpyrromethene (HMPM) (Figure 4) is a particularly instructive example since it (i) represents a model compound for the inner pyrrole rings and (ii) undergoes different types of hydrogen-bond interactions.[24,25] Monomeric HMPM forms an intramolecular hydrogen bond between the pyrrolenic and pyrrolic nitrogens, which may be comparable in strength to intra- and intermolecular hydrogen bonds in protein-bound tetrapyrroles.[24] The scaling factors for the N−H in-plane bending (ip) and out-of-plane (oop) force constants that are optimized for monomeric HMPM are, therefore, adopted for the calculations of the chromophores in phytochrome.[19] In HMPM dimers, the monomeric entities are oriented perpendicularly to each other and held together via intra- and intermolecular bonds. Here, force constant scaling is not sufficient for a satisfactory description of the vibrational spectra.[25] Instead, intra- and intermolecular coupling constants in the force field require some adjustments that are not transferable to other molecules. However, this failure of the force field scaling approach appears to be restricted to the rather unusual nonplanar hydrogen-bond geometries.

For molecules as large as tetrapyrroles, the number of normal modes is so high that an unambiguous assignment of the RR bands solely based on the comparison with the

calculated frequencies is not possible. Additional assignment criteria are required, which can be provided by calculated band intensities. These calculations are straightforward for Raman and IR intensities and allow for a semiquantitative prediction of the experimental intensities. Calculations of RR intensities are significantly more demanding. We have therefore evaluated the costs and benefits of RR intensity calculations using HMPM as a test molecule.[26] A particularly promising concept combines quantum mechanical methods with the use of experimental data. Within the framework of the so-called transform theory, the frequency dependence of the scattering tensor is obtained by the Kramers−Kronig transformation of the absorption band,[27] while the electronic transition dipole moments as well as the excited-state geometries are calculated by time-dependent DFT. However, even for a relatively "simple" molecule like HMPM, these calculations may be associated with substantial theoretical challenges, which in addition to the considerable computational costs represent serious obstacles for extending the approach to tetrapyrroles. On the other hand, the relative band intensities in the Raman spectra of tetrapyrroles obtained in resonance and preresonance with the Q-band display far-reaching similarities, evidently due to the low symmetry of the chromophore. Consequently, it appears to be justified to restrict the Raman intensity calculations to the off-resonance case, and in fact, the agreement with the experimental band intensities is comparable to that achieved for small molecules under nonresonant conditions.

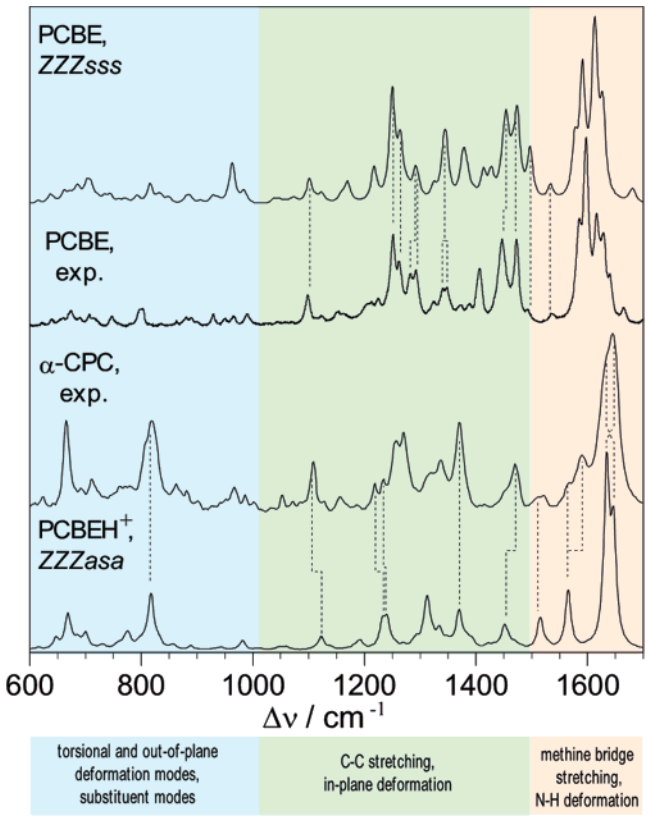

FIGURE 5. Raman spectra calculated for dimeric PCBE (*ZZZsss*) and monomeric $PCBEH^+$ (*ZZZasa*) compared with the experimental RR spectra of solid PCBE[30] and α-CPC.[34] The spectral regions dominated by various types of vibrational modes are shown by the shaded areas.

Potential and Limitations of the Theoretical Approach

The objective of the theoretical approach is to calculate Raman spectra of various tetrapyrrole geometries such that the comparison with the experimental RR spectra allows identification of the chromophore structures in the various states of phytochrome. However, is the accuracy of this approach sufficient and is it justified to extend conclusions drawn from *in vacuo* calculations to protein-bound tetrapyrroles? To explore the potential and limitations of the DFT calculations, we first consider phycocyanobilin (PCB). For this tetrapyrrole, experimental data are available for two different structures. The dimethyl ester derivative of PCB (PCBE) (Figure 4) in the solid state most likely adopts the same helical *ZZZsss* structure as biliverdin (BV) dimethyl ester, for which the crystal structure has been determined.[28]

NMR and circular dichroism studies of PCBE in solution have shown the coexistence of at least two diastereoisomers, a P-helical and an M-helical form,[29] and two tautomers with the either ring B or ring C being the pyrrolic ring. The calculated spectra of none of the monomeric PCBE forms provide a satisfactory description of the experimental Raman and IR spectra obtained from PCBE in the solid state or in concentrated solutions.[30] Under these conditions, PCBE is likely to form dimers via hydrogen-bond interactions involving the carbonyl functions and the NH groups of the terminal pyrrolidone and pyrrolone rings. There are a variety of possibilities how dimerization between two PCBE molecules may occur. The best agreement with the experimental spectra has been achieved for a C-pyrrolic tail-to-tail dimer (DD dimer) (Figures 4 and 5), a geometry that was calculated to be the most stable one and has also been found experimentally for a related tetrapyrrole.[31]

The second experimentally determined structure of PCB refers to the α-subunit of C-phycocyanin (α-CPC), an antenna pigment of cyanobacteria.[32] In this case, the crystal structure analysis indicates an extended *ZZZasa* configuration of the chromophore, and the close proximity of the nitrogen atoms of rings B and C to the carboxylate side chain of Asp87 suggests a protonated (cationic) form of PCB. The calculations, therefore, have been carried out for a protonated PCBE ($PCBEH^+$). The linkage to the protein was replaced by a hydrogen atom, and the propionic side chains were esterified to avoid hydrogen-bond interactions with the pyrrole rings. A chloride anion was placed between rings B and C in order to mimic the electrostatic interactions with Asp87. Also in this case, a very good agreement between the calculated and the experimental spectrum is obtained (Figure 5).[33] These findings indicate that (i) the performance of scaled quantum chemical force field calculations is comparable for tetrapyrroles as for the substantially smaller training molecules for which the scaling factors have been opti-

mized and (ii) calculated Raman intensities for open-chain tetrapyrroles provide a good description for the experimental RR intensities.

The most severe approximation of the calculations refers to the neglect of the protein environment, which may affect the electron density distribution and the conformation of the chromophore. A chromophore structure stabilized in the protein pocket may not necessarily correspond to an equilibrium geometry *in vacuo*. Such effects may be particularly strong for modes below 1000 cm^{-1}, which include torsional and deformation coordinates as well as internal coordinates of the pyrrole substituents (Figure 5). In fact, *in vacuo* equilibrium geometries of tetrapyrroles with different conformations and functionalization of the propionic side chains afford spectral differences in this region but do not influence the band pattern above 1200 cm^{-1}. On the other hand, more drastic structural differences on the level of the methine bridge configuration (*Z*/*E*) and conformation (*s*/*a*) and the protonation state of the ring B and C nitrogens are clearly reflected in the frequency range between 1200 and 1700 cm^{-1}.[19] For the unprotonated (neutral) *ZZZsss* configuration of dimeric PCBE and the protonated (cationic) *ZZZasa* configuration of the PCB in α-CPC, these differences are very well reproduced by the calculations. This high-frequency region includes an unambiguous spectral marker for the protonation state of tetrapyrroles: in the protonated (cationic) form, the inner rings B and C become essentially equivalent and their N−H ip modes give rise two bands between 1500 and 1600 cm^{-1}.[14] The high-frequency component, typically found at 1550−1590 cm^{-1}, has a considerable RR intensity and shifts down by ca. 500 cm^{-1} upon H/D exchange. For nonprotonated (neutral) tetrapyrroles, the H/D isotopic effects in this region are relatively small.

From these studies, we conclude that it is only the high-frequency region (1200−1700 cm^{-1}) that can currently be interpreted in a reliable manner on the basis of the quantum chemical spectra calculation. The analysis of this spectral region then allows determination of the methine bridge configuration and conformation, as well as the protonation state of the tetrapyrroles.

Interpretation of the Resonance Raman Spectra of Phytochromes: The Parent State, Pr

A large set of experimental RR data is available for plant phytochrome phyA, which contains phytochromobilin (PΦB) as the natural chromophore (Figure 2). The 65-kDa variant of phyA lacking the kinase domain can be expressed and then assembled either with PΦB or with PCB. The RR spectrum of the phyA(PΦB) adduct is virtually identical to that of the full-length protein indicating that the kinase domain does not affect the structure of the chromophore pocket. Also the Pr states of the PΦB and PCB adducts display very similar RR spectra, and the few differences can readily be attributed to the different ring D substituents, that is, a vinyl and an ethyl group in PΦB and PCB, respectively (Figures 2 and 6).[17] Thus, it is concluded that both chromophores adopt the same methine bridge configuration and conformation. Moreover, the chromophore is protonated as can be unambiguously inferred from the band of 1574 cm^{-1} (Figure 6), which disappears upon H/D exchange.[14]

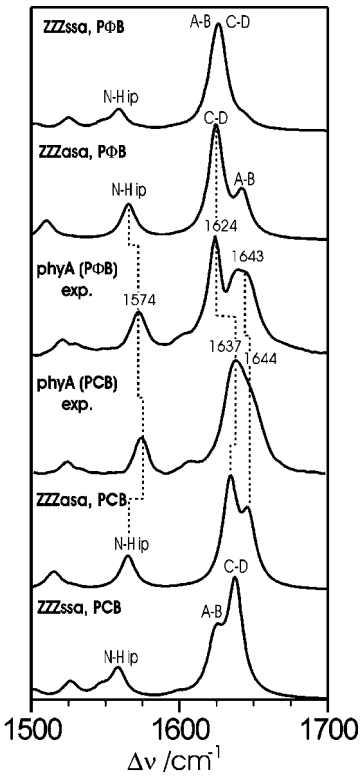

FIGURE 6. Calculated Raman spectra of protonated PΦB (top) and PCB (bottom) in the *ZZZssa* and *ZZZasa* configurations, compared with the experimental RR spectra of the Pr state of 65-kDa phyA, reconstituted with PΦB and PCB.[17] A−B and C−D denote the C=C stretching modes at the methine bridges between rings A and B and C and D, respectively.

The RR spectrum of the Pr state of phyA(PCB) reveals striking similarities with that of the *ZZZasa* chromophore in α-CPC, whereas the crystal of the Pr state of the BV-binding phytochrome DrBphP has demonstrated a *ZZZssa* configuration (Figures 2 and 3).[4] The analysis of the RR spectra resolves this contradiction. First, only for the *ZZZasa* but not for the *ZZZssa* geometry, the calculated spectra reproduce the double-banded structure of the prominent peak as well as the 13-cm^{-1} upshift of the strongest band component from phyA(PΦB) to phyA(PCB) (Figure 6). Second, the isotopic shifts for PCB deuterated at the *C-D* methine bridge (Figure 7) and for ^{13}C-substitution at the A−B bridge (spectra not shown) are only consistent with the calculated spectra for the *ZZZasa* geometry. Also other tetrapyrrole geometries, including those previously suggested for the Pr state, do not afford a satisfactory description of the experimental spectra.[19] These findings suggest that unlike in DrBphP, the chromophore in phyA is in the *ZZZasa* configuration. This surprising difference might be related to the different location of the tetrapyrrole-binding cysteines in the chromophore pocket, that is, Cys24 for DrBphP and Cys323

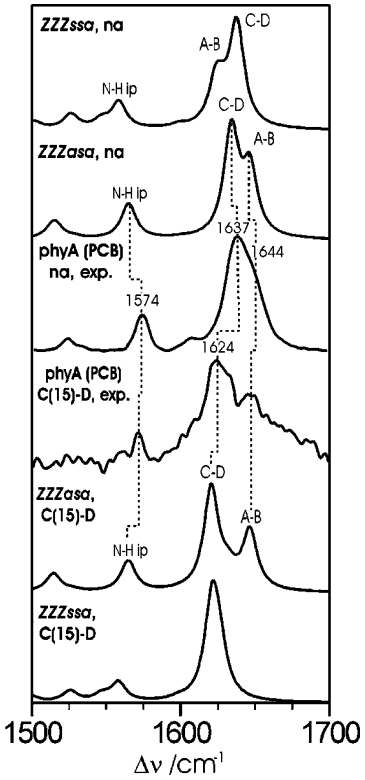

FIGURE 7. Calculated Raman spectra of the *ZZZssa* and *ZZZasa* configurations of protonated, unlabeled (natural abundance, na) PCB (top) and protonated PCB deuterated at the methine bridge C−D [C(15)−D] (bottom) compared with the experimental RR spectra of the 65-kDa fragment of phyA reconstituted with the unlabeled and C(15)-deuterated PCB (unpublished results). A−B and C−D denote the C═C stretching modes at the methine bridges between rings A and B and C and D, respectively.

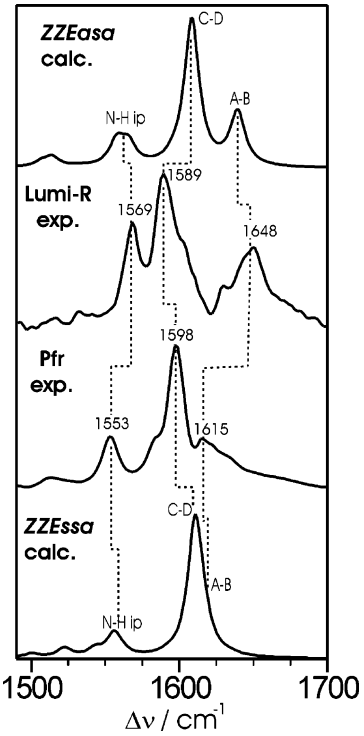

FIGURE 8. Calculated Raman spectra of protonated PΦB in the *ZZEasa* (top) and *ZZEssa* (bottom) configurations compared with the experimental RR spectra of Lumi-R and Pfr of native phyA.[19]

for phyA. It is tempting to generalize this conclusion in view of the far-reaching spectral similarities between DrBphP and Agp1, a BV-binding phytochrome from *Agrobacterium tumefaciens*, on the one hand (ref 16, unpublished results), and phyA and Cph1, a PCB-binding phytochrome from the *Cyanobacterium syneccocystis*, on the other hand:[18] the chromophore in the Pr state in BV-binding phytochromes adopts a *ZZZssa* geometry but a *ZZZasa* geometry in PΦB- and PCB-binding phytochromes (Figure 2).

Methine Bridge Isomerizations during the Pr to Pfr Photoconversion

Early NMR spectroscopic studies of proteolytic phytochrome fragments have indicated a *Z* and *E* configuration of the C−D methine bridge in the Pr and Pfr state, respectively.[3] Thus, the primary photochemical process of Pr was assumed to be a *Z*/*E* isomerization of the C−D methine bridge. It has been further suggested that the double bond isomerization is associated with a rotation of the adjacent single bond (*s*/*a*).[11] Hence, the chromophore in the first intermediate state of the Pr → Pfr photoconversion of phyA that can be cryogenically trapped, Lumi-R, should adopt either the *ZZEasa* or *ZZEass* configuration. Upon comparison with the experimental spectrum of Lumi-R, the *ZZEass* configuration can be ruled out whereas a better agreement is found with the spectrum calculated for the *ZZEasa* configuration, implying that the primary photochemical event is most likely restricted to the *Z* to *E* isomerization (Figure 8).[19]

The experimental RR spectrum of Pfr displays quite substantial differences compared with Lumi-R indicating major structural changes of the chromophore and its interactions with the protein during the thermal relaxations steps from Lumi-R to Pfr.[35] Specifically, we note a 33 cm^{-1} downshift of the 1648 cm^{-1} band that originates from the C═C stretching of the A−B methine bridge (Figure 8).[19] Such a large downshift can only be reproduced by the calculated spectrum of the geometry in which the A−B methine bridge geometry is altered, that is, the *ZZEssa* configuration.[19] This conclusion is further supported by the RR spectra of phyA(PCB) adducts including isotopically labeled chromophores. It may be that the A−B single bond rotation is not complete or that the (partial) *s*/*a* isomerization is accompanied by further changes in the protein−chromophore interactions since the overall agreement between calculated and experimental spectra is not as good as in the case of the Pr state.

Changes of the Protonation State during the Pr to Pfr Photoconversion

All phytochrome states discussed so far, that is, Pr, Lumi-R, and Pfr, exhibit a protonated chromophore as indicated by the characteristic N−H ip mode. This is also true for the Meta-Ra state,[14] whereas the Meta-Rc state displays a more complex behavior. For the BV-binding phyto-

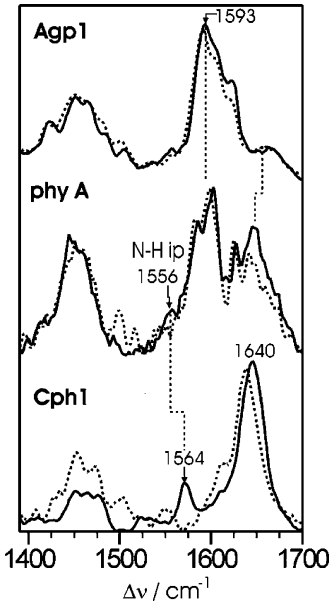

FIGURE 9. Experimental RR spectra of the Meta-Rc states of Agp1, phyA, and Cph1. The solid and dotted lines refer to the spectra obtained from samples in H_2O and D_2O, respectively.

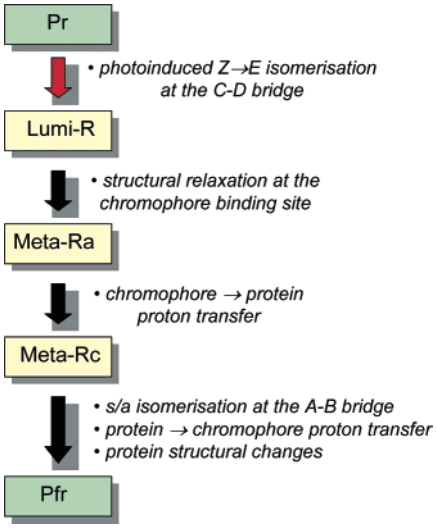

FIGURE 10. Model for the structural changes of the Pr to Pfr photoconversion of phytochromes.

chromes like Agp1 and DrBphP, the spectra of these intermediates lack the characteristic protonation marker bands and display far-reaching similarities with the spectrum of the unprotonated BV in the *ZZE* configuration (Figure 9) (ref 16, unpublished results). In fact, flash photolysis experiments on Agp1 reveal a substantial kinetic isotope effect for the formation of Meta-Rc indicating that the deprotonation of the chromophore is rate-limiting.[16] The chromophore deprotonation is linked to the translocation of the proton to the external medium where it can be detected by pH indicators. The subsequent reprotonation of the chromophore in Pfr occurs with the same time constant as the proton reuptake from the external medium.

Most of the amino acids that constitute the chromophore pocket in the Pr state of DrBphP (ref 4; Figure 3) are well conserved. Thus, the crystal structure determined for DrBphP may be a good model for the related BV-binding phytochrome Agp1, and many structural features are likely to be similar also for other phytochromes. Accordingly, the chromophore is involved in an extended hydrogen-bond network, which comprises Asp207 (Asp197) and His260 (His250) in DrBphP (Agp1). Although these amino acid residues do not directly interact with the pyrrole nitrogens of the chromophore, the substitution by alanine substantially lowers the pK_a in the Pr state in Agp1 from 11.1 to 8.2 (His250Ala) and 7.2 (Asp197Ala).[36] Evidently, the overall electrostatic field in the chromophore pocket rather than the specific interaction with an individual amino acid side chain controls the protonation of the chromophore, which is essential for the photoisomerization of the chromophore. The second function of Asp197 and His250 is related to the transient proton translocation and the coupled conformational changes. In Asp197Ala but not in His250Ala, the proton release to the external medium is inhibited indicating that the Asp197 carboxylate side chain, which in the crystal structure is exposed to the solvent, is an essential component for the proton translocation chain. In Asp197Ala and His250Ala the proton reuptake is blocked, which is consistent with the inhibition of the Meta-Rc to Pfr reaction step. Thus, His250 appears to be essential for the chromophore and protein structural changes associated with the Pfr formation. These structural changes include major polypeptide rearrangements that are detectable by size exclusion chromatography.[35]

A transient proton release, as well as significant kinetic isotope effects, has also been found for the Pr to Pfr photoconversion of the PCB-binding phytochrome Cph1.[18] However, in this case, the Meta-Rc state that is cryogenically trapped provides the characteristic RR signature of a protonated chromophore (Figure 9). Conversely, the RR spectrum of Meta-Rc of phyA including the PΦB chromophore is dominated by nonprotonated chromophore species, which is in line with earlier suggestions by Kitagawa and co-workers.[12] These findings indicate that a protonation equilibrium of the Meta-Rc state is a common property of all phytochromes although the position of the equilibrium may differ for cryogenically trapped states among the various phytochromes. Evidently, the protonation equilibrium of the Meta-Rc sensitively depends on details of the protein environment.

Conclusions and Outlook

The mechanistic picture that is derived from the spectroscopic data for the Pr to Pfr transformation appears to be common to all phytochromes studied so far, regardless of the chromophore structure in the initial state (Figure 10). The process that is initiated by a *Z*/*E* photoisomerization of the C−D methine bridge yields a *ZZEssa* and a *ZZEasa* configuration in the Lumi-R state of DrBphP and phyA, respectively. The subsequent thermal relaxation steps then involve a transient deprotonation of the chromophore in the Meta-Rc state, which is crucial for the final protein structural rearrangement in the transition to Pfr.

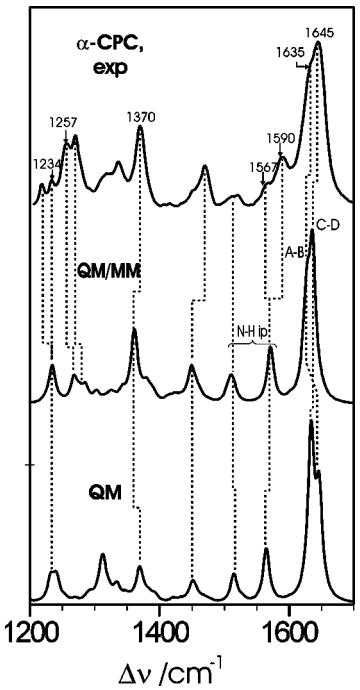

FIGURE 11. Experimental RR spectrum of α-CPC[34] compared with the calculated Raman spectra obtained by a QM/MM (B3LYP/6-31G*/CHARMM) treatment of the protein and by a QM calculation of the chromophore *in vacuo* (unpublished results).

Presumably, this reaction step also involves the (partial) single bond rotation of the A−B methine bridge.

Although the quantum chemical calculations of Raman spectra have contributed substantially to the elucidation of the molecular events in phytochrome, the present approach does not allow a comprehensive extraction of structural information from the experimental spectra. The main limitation lies in the unavoidable neglect of the protein environment. To overcome this restriction, hybrid methods may be employed, consisting of a combination of quantum mechanics (QM) calculations and molecular dynamics/molecular mechanics (MD/MM) simulations.[36] These methods represent a promising conceptual approach for calculating spectral properties of cofactors in proteins since it allows an accurate treatment of the chromophore by QM (e.g., DFT) methods and a less accurate but computationally cheaper description of the environment by an empirical force field. The potential of this approach is demonstrated for α-CPC in Figure 11 (unpublished results). The Raman spectrum calculated by the QM/MM approach provides an improved description of the experimental RR spectrum. Specifically, we note that the intensity distribution of the most prominent double-banded peak at 1645 cm^{-1}, as well as the vibrational structure between 1200 and 1400 cm^{-1}, is much better matched than that for the pure QM calculations. With the availability of the crystal structure of DrBphP,[4] it is now possible to apply the QM/MM approach to phytochrome such that one may expect to derive more structural details from the RR spectra in the future.

The work was supported by the Deutsche Forschungsgemeinschaft (Grant Sfb 498).

References

(1) Briggs, W. R.; Spudich, J. L. *Handbook of Photosensory Receptors*; Wiley: Weinheim, Germany, 2005.
(2) Lamparter, T. Evolution of cyanobacterial and plant phytochromes. *FEBS Lett.* **2004**, *573*, 1−5.
(3) Rüdiger, W.; Thümmler, F.; Cmiel, E.; Schneider, S. Chromophore structure of the physiologically active form (Pfr) of phytochrome. *Proc. Natl. Acad. Sci. U.S.A.* **1983**, *80*, 6244−6248.
(4) Wagner, J. R.; Brunzelle, J. S.; Forest, K. T.; Vierstra, R. D. A light-sensing knot revealed by the structure of the chromophore-binding domain of phytochrome. *Nature* **2005**, *438*, 325−331.
(5) Fodor, S. P. A.; Lagarias, J. C.; Mathies, R. A. Resonance Raman-spectra of the Pr-form of phytochrome. *Photochem. Photobiol.* **1988**, *48*, 129−136.
(6) Tokutomi, S.; Mizutani, Y.; Anni, H.; Kitagawa, T. Resonance Raman-spectra of large pea phytochrome at ambient-temperature - difference in chromophore protonation between red-absorbing and far red-absorbing forms. *FEBS Lett.* **1990**, *269*, 341−344.
(7) Hildebrandt, P.; Hoffmann, A.; Lindemann, P.; Heibel, G.; Braslavsky, S. E.; Schaffner, K.; Schrader, B. Fourier-transform resonance Raman spectroscopy of phytochrome. *Biochemistry* **1992**, *31*, 7957−7962.
(8) Althaus, T.; Eisfeld, W.; Lohrmann, R.; Stockburger, M. Application of Raman spectroscopy to retinal proteins. *Isr. J. Chem.* **1995**, *35*, 227−251.
(9) Naumann, H.; Engelhard, M.; Murgida, D. H.; Hildebrandt, P. Time-resolved resonance Raman spectroscopy of sensory rhodopsin II from *Natronobacterium pharaonis*. *J. Raman Spectrosc.* **2006**, *37*, 436−441.
(10) Fodor, S. P. A.; Lagarias, J. C.; Mathies, R. A. Resonance Raman analysis of the Pr and Pfr forms of phytochrome. *Biochemistry* **1990**, *29*, 11141−11146.
(11) Andel, F., III; Lagarias, J. C.; Mathies, R. A. Resonance Raman analysis of chromophore structure in the lumi-R photoproduct of phytochrome. *Biochemistry* **1996**, *35*, 15997−16008.
(12) Mizutani, Y.; Tokutomi, S.; Aoyagi, K.; Horitsu, K;, Kitagawa, T. Resonance Raman-study on intact pea phytochrome and its model compounds - evidence for proton migration during the phototransformation. *Biochemistry* **1991**, *30*, 10693−10700.
(13) Matysik, J.; Hildebrandt, P.; Schlamann, W.; Braslavsky, S. E.; Schaffner, K. Fourier-transform resonance Raman spectroscopic study of the intermediate states of phytochrome. *Biochemistry* **1995**, *34*, 10497−10507.
(14) Kneip, C.; Hildebrandt, P.; Schlamann, W.; Braslavsky, S. E.; Mark, F.; Schaffner, K. Protonation state and structural changes of the tetrapyrrole chromophore during the $P_r \rightarrow P_{fr}$ phototransformation of phytochrome. A resonance Raman spectroscopic study. *Biochemistry* **1999**, *38*, 15185−15192.
(15) Kneip, C.; Schlamann, W.; Braslavsky, S. E.; Hildebrandt, P. Resonance Raman spectroscopic study of the tryptic 39kDa fragment of phytochrome. *FEBS Lett.* **2000**, *482*, 252−256.
(16) Borucki, B.; von Stetten, D.; Seibeck, S.; Lamparter, T.; Michael, N.; Mroginski, M. A.; Otto, H.; Murgida, D. H.; Heyn, M. P.; Hildebrandt, P. Light-induced proton release of phytochrome is coupled to the transient deprotonation of the tetrapyrrole chromophore. *J. Biol. Chem.* **2005**, *280*, 34358−34364.
(17) Kneip, C.; Mozley, D.; Hildebrandt, P.; Gärtner, W.; Braslavsky, S. E.; Schaffner, K. Effect of chromophore exchange on the resonance Raman spectra of recombinant phytochromes. *FEBS Lett.* **1997**, *414*, 23−26.
(18) Remberg, A.; Lindner, I.; Lamparter, T.; Hughes, J.; Kneip, C.; Hildebrandt, P.; Braslavsky, S. E.; Gärtner, W.; Schaffner, K. Raman spectroscopic and light-induced kinetic characterization of a recombinant phytochrome of the cyanobacterium *Synechocystis*. *Biochemistry* **1997**, *36*, 13389−13395.
(19) Mroginski, M. A.; Murgida, D. H.; von Stetten, D.; Kneip, C.; Mark, F.; Hildebrandt, P. Determination of the chromophore structures in the photoinduced reaction cycle of phytochrome. *J. Am. Chem. Soc.* **2004**, *126*, 16734−16735.
(20) Rauhut, G.; Pulay, P. Transferable scaling factors for density functional derived vibrational force fields. *J. Phys. Chem.* **1995**, *99*, 3093−4000.
(21) Magdo, I.; Nemeth, K.; Mark, F.; Hildebrandt, P.; Schaffner, K. Calculation of vibrational spectra of linear tetrapyrroles. Global sets of scaling factors for force fields derived by ab initio and density functional theory methods. *J. Phys. Chem. A* **1999**, *103*, 289−303.
(22) Mroginski, M. A.; Murgida, D. H.; Hildebrandt, P. Calculation of vibrational spectra of linear tetrapyrroles. 4. Methine bridge C−H out-of-plane modes. *J. Phys. Chem. A* **2006**, *110*, 10564−10574.

(23) Del Bene, J. E.; Person, W. B.; Szczepaniak, K. Properties of hydrogen-bonded complexes obtained from B3LYP functional with 6-31G(p,d) and 6-31+G(d,p) basis set: Comparison with MP2/6-31+G(d,p) results and experimental data. *J. Phys. Chem.* **1995**, *99*, 10705−10707.
(24) Mroginski, M. A.; Németh, K.; Magdó, I.; Müller, M.; Robben, U.; Della Védova, C.; Hildebrandt, P.; Mark, F. Calculation of vibrational spectra of linear tetrapyrroles. 2. Resonance Raman spectra of hexamethyl pyrromethene monomers. *J. Phys. Chem. B* **2000**, *104*, 10885−10899.
(25) Mroginski, M. A.; Németh, K.; Bauschlicher, T.; Klotzbücher, W.; Goddard, R.; Heinemann, O.; Hildebrandt, P.; Mark, F. Calculation of vibrational spectra of linear tetrapyrroles. 3. Hydrogen bonded hexamethylpyrromethene dimers. *J. Phys. Chem. A* **2005**, *109*, 2139−2150.
(26) Mroginski, M. A.; Hildebrandt, P.; Kneip, C.; Mark, F. Excited state geometry calculations and the resonance Raman spectrum of hexamethylpyrromethene. *J. Mol. Struct.* **2003**, *661*−*662*, 611−624.
(27) Rush, T. S., I.; Peticolas, W. L. Ab initio calculation of resonance Raman spectra of uracil, 1-methyluracil, and 5-methyluracil. *J. Phys. Chem.* **1995**, *99*, 14647−14658.
(28) Sheldrick, W. S. Molecular structures of linear polypyrrolic pigments. *Isr. J. Chem.* **1983**, *23*, 155−166.
(29) Knipp, B.; Muller, M.; Metzler-Nolte, N.; Balaban, T. S.; Braslavsky, S. E.; Schaffner, K. NMR verification of helical conformations of phycocyanobilin in organic solvents. *Helv. Chim. A* **1998**, *81*, 881−888.
(30) Hildebrandt, P.; Kneip, C.; Matysik, J.; Nemeth, K.; Magdo, I.; Mark, F.; Schaffner, K. Vibrational analysis of linear tetrapyrroles. implications for interpreting the resonance Raman spectra of phytochrome. *Rec. Res. Dev. Phys. Chem.* **1999**, *3*, 63−77.
(31) Kratky, C.; Falk, H.; Grubmayr, K. The crystal and molecular-structures of the diastereomeric (4*Z*)-3-oxo-2,3-dihydrobilatrienes-abc and (4*E*)-3-oxo-2,3-dihydrobilatrienes-abc. *Monatsh. Chem.* **1985**, *116*, 745−760.
(32) Duerring, M.; Huber, R.; Bode, W. Refined three-dimensional structure of phycoerythrocyanin from the cyanobacterium *Mastigocladus laminosus* at 2.7 Å. *J. Mol. Biol.* **1990**, *211*, 633−644.
(33) Kneip, C.; Nemeth, K.; Mark, F.; Hildebrandt, P.; Schaffner, K. Interpretation of the resonance Raman spectra of linear tetrapyrroles based on dft calculations. implications for the structure and protonation state of the chromophore in phytochrome. *Chem. Phys. Lett.* **1999**, *311*, 479−484.
(34) Kneip, C.; Hildebrandt, P.; Foerstendorf, H.; Siebert, H.; Parbel, A.; Scheer, H. FT-NIR resonance Raman spectroscopic study of the α-subunit of phycoerythrocyanin and phycocyanin from the cyanobacterium *Mastigocladus laminosus*. *J. Raman Spectrosc.* **1998**, *29*, 939−944.
(35) von Stetten, D.; Mroginski, M. A.; Murgida, D. H.; Hildebrandt, P.; Borucki, B.; Seibeck, S.; Heyn, M. P.; Scheerer, P.; Krauss, N.; Michael, N.; Lamparter, T. Highly conserved residues D197 and H250 in the chromophore binding pocket of Agp1 phytochrome control the proton affinity of the chromophore and are essential for the formation of the Pfr form. *J. Biol. Chem.* **2007**, in press.
(36) Shurki, A.; Warshel, A. Structure/function correlations of proteins using MM, QM/MM, and related approaches: Methods, concepts, pitfalls, and current progress. *Adv. Protein Chem.* **2003**, *66*, 249−313.

AR6000523